

Hint of non-standard MSW dynamics in solar neutrino conversion

Antonio Palazzo

*Excellence Cluster Universe, Technische Universität München,
Boltzmannstraße 2, D-85748, Garching, Germany*

(Dated: April 27, 2019)

Motivated by the recent low-threshold measurements of the solar ^8B neutrino spectrum performed by Borexino, Super-Kamiokande and the Sudbury Neutrino Observatory – all now monitoring the transition regime between low-energy (vacuum-like) and high-energy (matter-dominated) flavor conversions – we consider the role of sub-dominant dynamical terms induced by new flavor-changing interactions. We find that the presence of such perturbations with strength $\sim 10^{-1}G_F$ is favored by the analysis, being able to describe the anomalous behavior of the solar neutrino spectrum suggested by the new results, which show no sign of the typical low-energy upturn predicted by the standard MSW mechanism. Our findings, if interpreted as a positive indication, provide a hint of such new effects at the $\sim 2\sigma$ level.

PACS numbers: 14.60.Pq, 13.15.+g

I. INTRODUCTION

One of the most important achievements in the understanding of neutrino properties is undoubtedly constituted by the (indirect) proof of the existence of matter effects in solar neutrino flavor conversion, as predicted by the Mikheev-Smirnov-Wolfenstein (MSW) mechanism [1, 2]. In fact, the explanation of the solar neutrino problem requires a peculiar energy dependence of the electron neutrino survival probability (P_{ee}), which is elegantly provided by MSW transitions in adiabatic regime [3]. At low energies ($E \lesssim 1$ MeV) matter effects play a negligible role and a (averaged) vacuum-like behavior emerges, giving rise to $P_{ee} \sim 1/2$, in agreement with the determinations of the Gallium experiments SAGE [4] and GALLEX/GNO [5–7]. At high energies ($E \sim 10$ MeV) matter effects dominate, leading to a much stronger signal suppression ($P_{ee} \sim 1/3$), as confirmed by the accurate boron neutrino (^8B ν) measurements performed by SNO [8–13] and Super-Kamiokande [14–16]. This behavior is indirectly corroborated by the Chlorine [17] experiment, whose total rate gets two (inseparable) contributions from both low- and high-energy neutrinos, and has recently received direct confirmation by the real time measurements performed by Borexino [18, 19], able to monitor separately both regimes. Such a picture is now considered a standard framework thanks to the spectacular results of the reactor experiment KamLAND [20–23], which has provided the unique opportunity to measure the solar mass-mixing parameters in vacuum, independently of dynamical effects induced by the neutrino interaction with matter.

It is well known [1, 24–26] that neutrino non-standard interactions, described by low-energy four-fermion operators $\mathcal{O}_{\alpha\beta} \sim \bar{\nu}_\alpha \nu_\beta \bar{f} f$ of sub-weak strength $\epsilon_{\alpha\beta} G_F$, especially of the flavor-changing type ($\alpha \neq \beta$), can profoundly modify the flavor conversion process. Interestingly, such new interactions may produce appreciable deviations *only* in the intermediate energy region [27] describing the transition between vacuum-like and matter-

dominated conversions, without affecting the well established behaviors observed at low and high energies. Therefore, the accurate observation of this energy region is of crucial importance for pinning down potential new physics beyond the Standard Model.

Intriguingly, the first low-threshold ^8B ν measurements performed by Borexino [19] and by the SNO low energy threshold analysis [13] (LETA), together with those provided by the older (SK-I [15]) and newer (SK-III [16]) Super-Kamiokande data, indicate an anomalous behavior, showing no evidence of the low-energy up-turn of the spectrum predicted by the standard MSW mechanism. This new circumstance suggests that new interactions may be effectively at work, affecting the conversion process of solar neutrinos in an observable way. In this paper we quantify such an expectation by showing that, with the inclusion of the new spectral information, the solar sector data (solar+KamLAND) display a non-negligible preference for NSI, disfavoring the standard MSW picture at the $\sim 2\sigma$ level.

II. NOTATION

For a system of two active neutrinos, in the flavor basis, the evolution is governed by a Schroedinger like equation

$$i \frac{d}{dx} \begin{pmatrix} \nu_e \\ \nu_a \end{pmatrix} = H \begin{pmatrix} \nu_e \\ \nu_a \end{pmatrix}, \quad (1)$$

where ν_a is a linear combination of ν_μ and ν_τ , and H is the total Hamiltonian

$$H = H_{\text{kin}} + H_{\text{dyn}}^{\text{std}} + H_{\text{dyn}}^{\text{NSI}}, \quad (2)$$

split in the sum of the kinetic term, the standard MSW term [1, 2], and a new NSI-induced term. The kinetic term reads $H_{\text{kin}} = UKU^\dagger$, where U is the 2×2 mixing matrix depending on the mixing angle θ_{12} , and K is the diagonal matrix of wavenumbers $k_i = m_i^2/2E$ (m_i and E being the neutrino squared masses and energy respectively). In the presence of ordinary matter, the standard

electroweak theory predicts $H_{\text{dyn}}^{\text{std}} = \text{diag}(V, 0)$, where $V(x) = \sqrt{2}G_F N_e(x)$ is the effective potential induced by the charged current ν_e interaction with the electrons having number density $N_e(x)$. For interactions with a background fermion f having number density $N_f(x)$, the new term can be expressed as [28]

$$H_{\text{dyn}}^{\text{NSI}} = \sqrt{2}G_F N_f(x) \begin{pmatrix} 0 & \epsilon \\ \epsilon & \epsilon' \end{pmatrix}, \quad (3)$$

where ϵ and ϵ' are two effective parameters which, restricting to the case of flavor-changing interactions with d -quarks, are related to the fundamental vectorial coupling $\epsilon_{\alpha\beta}^{dV}$ as [28]

$$\epsilon = \epsilon_{e\mu}^{dV} \cos \theta_{23} - \epsilon_{e\tau}^{dV} \sin \theta_{23}, \quad (4)$$

$$\epsilon' = -\epsilon_{\mu\tau}^{dV} \sin 2\theta_{23}, \quad (5)$$

where θ_{23} is the atmospheric mixing angle. Taking into account the strong upper bounds on $\epsilon_{\mu\tau}^{dV}$ deriving from the atmospheric data analysis [29, 30], we can safely neglect the diagonal effective coupling ϵ' . Therefore, the conversion of solar neutrinos is described by the mass-squared splitting $\Delta m^2 = m_2^2 - m_1^2$, the mixing angle θ_{12} , and the effective parameter ϵ .

III. NUMERICAL RESULTS

In our analysis we have included the data from Homestake [17], SAGE [4] and GALLEX/GNO [5–7], SK-I [15], the third SNO phase [12], and the Borexino ${}^7\text{Be}$ data [18]. In addition, we have incorporated the new spectral information provided by SNO-LETA [13], SK-III [16], and the ${}^8\text{B}$ Borexino data [19]. We have also included the latest KamLAND results [23]. For the sake of precision, we have incorporated both standard and non-standard

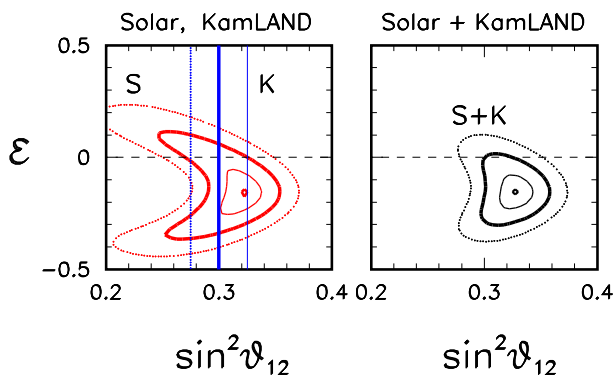


FIG. 1: Region allowed, after marginalization of Δm^2 as constrained by KamLAND, separately (left panel) by solar (S) and KamLAND (K) data and by their combination (right panel). The contours refer to $\Delta\chi^2 = 1$ (thin solid line), $\Delta\chi^2 = 4$ (thick solid line), and $\Delta\chi^2 = 9$ (dotted line).

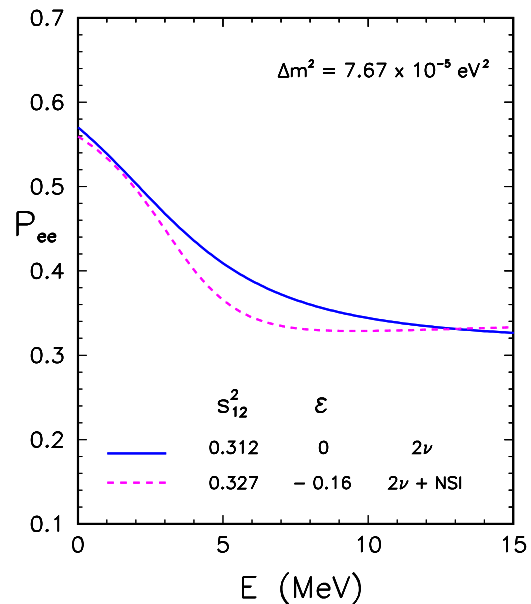


FIG. 2: Solar ν_e survival probability (averaged over the ${}^8\text{B}$ ν production region) for the best fit points obtained with (dashed line) and without (solid line) NSI effects.

matter effects also in the KamLAND analysis. However, due to the low density of the Earth's crust, both have only a negligible effect for the range of parameters we are considering. Therefore, the constraints obtained from KamLAND do not depend on NSI. We also included NSI effects in the propagation of solar neutrinos in the Earth which, as noted in [27], can slightly modify the regeneration effect.

In Fig. 1, we display the result of the analysis, by showing the allowed region (at the 1σ and 2σ level) in the plane charted by $[\sin^2 \theta_{12}, \epsilon]$, after marginalization of Δm^2 , which in practice is fixed by KamLAND. In the first panel we show separately the region determined by solar and KamLAND data. As already noticed in [31], for negative values of ϵ the solar data tend to prefer larger values of the mixing angle, with an improved agreement with KamLAND. We also notice that, the solar data taken *alone* now tend to prefer non-zero NSI. As we will discuss below, this behavior can be traced to the anomalous energy spectrum suggested by the present data. In the right panel we report the region allowed by the combination of solar and KamLAND data. This plot shows that the standard MSW case ($\epsilon = 0$) is disfavored almost at the 2σ level; more exactly we find $\Delta\chi^2 \simeq 3.6$, corresponding to 1.9σ . The best fit is obtained for the effective coupling¹ $\epsilon \simeq -0.16$, which, assuming maxi-

¹ Interestingly, a similar preference for flavor-changing NSI in the (ν_μ, ν_τ) sector has been evidenced in connection with the mis-

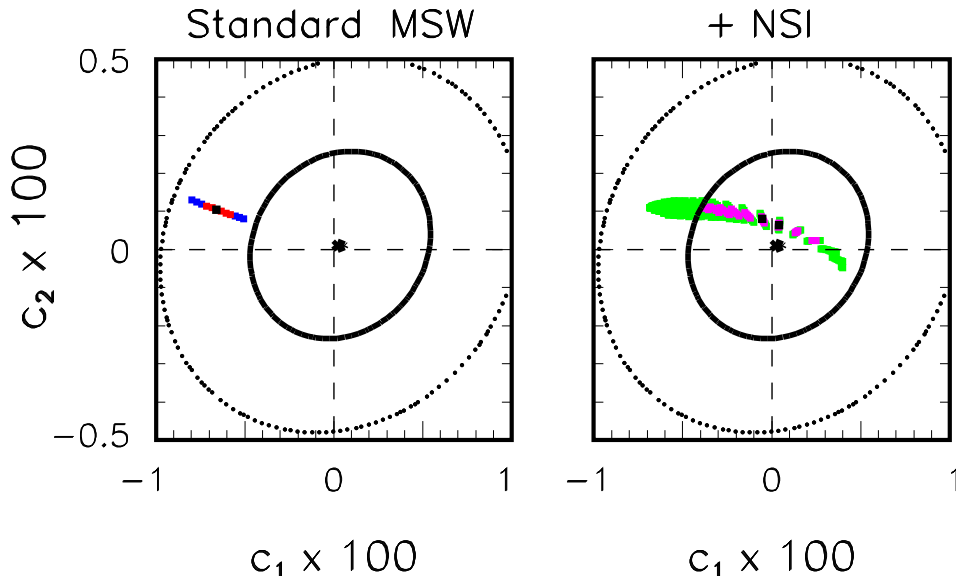


FIG. 3: The (ellipse-like) region determined by all data sensitive to ${}^8\text{B}$ neutrinos is reported in both panels. In the left (right) panel the region spanned by the theoretical model in the absence (presence) of NSI effects is superimposed. Both experimental and theoretical regions are plotted for $\Delta\chi^2 = 1, 4$.

mal atmospheric mixing [34], corresponds to a difference $\epsilon_{e\tau}^{dV} - \epsilon_{e\mu}^{dV} = 0.23$, well compatible with the existing experimental bounds [35].

For definiteness, we have focused on the case of interactions with d-type quarks. However, the essence of our results is unaltered if interactions with u-type quarks or electrons are considered. In all cases the absence of non-standard effects is disfavored at the same statistical level. What changes is the best-fit value of ϵ , as can be expected from the proportionality of the new dynamical term to the fermion number density [see eq. (3)].

IV. DISCUSSION

In Fig. 2 we show the solar ν_e survival probability (averaged over the ${}^8\text{B}$ ν production region) as a function of the neutrino energy, for the best fit points obtained with or without NSI, respectively. In both cases the mass squared splitting is $\Delta m^2 = 7.67 \times 10^{-5} \text{eV}^2$, while the best fit values of $\sin^2 \theta_{12}$ are slightly different, as can be understood from the second panel of Fig. 1. It is evident how in the presence of NSI, the survival probability exhibits a distinctive flat behavior for $E \gtrsim 7$ MeV, in contrast with the standard MSW case which, in the same energy range, presents a negative slope.

To clarify the role of the spectral information in favoring the flatter NSI solution, following [13], we parametrize the survival probability (averaged over daytime and nighttime²) as a second order polynomial

$$P_{ee}(E) = c_0 + c_1(E - E_0) + c_2(E - E_0)^2 \quad (6)$$

where $E_0 = 10$ MeV approximately represents the value of the energy where the ${}^8\text{B}$ ν experiments are most sensitive. We have extracted the three coefficients from the combination of all the high energy experiments, taking into account their sensitivities. For SNO LETA this extraction is not feasible as detailed information on the bin-to-bin correlations of the spectrum is not available, and we have used directly the coefficient's information provided by the collaboration itself [13].

In both panels of Fig. 3 we report the ellipse-like region obtained by projecting the 3-dimensional allowed region onto the 2-dimensional parameter space of the two coefficients c_1 and c_2 , which encode the deviations from flatness. The contours correspond to the 1σ (continuous curve) and 2σ (dotted curve) level. The best fit coincides with the origin of the axes signaling a clear preference for a flat spectrum. In the left panel we superimpose the region spanned in the space of these two coefficients by the theoretical model in the absence of

match of the atmospheric mass-squared splitting observed, respectively, in neutrino and antineutrino measurements by MINOS [32, 33].

² Hereafter, we neglect the small deviations induced on the (night-time) survival probability due to the different latitudes of the three detectors Borexino, SNO and SK. We have checked that this approximation does not alter our conclusions.

NSI, at the 1σ and 2σ level. From this plot we learn that the standard MSW mechanism corresponds to a very well definite region in this plane: the variation of θ_{12} in the range allowed by the data produces only a modest excursion from the best fit point, which is obtained for a negative value of c_1 , corresponding to the expected low-energy up-turn of the survival probability. The value of the experimental $\Delta\chi^2 \sim 2.1$ assumed in this point provides a quantitative measure of the slight disagreement among theory and data. In the right panel we superimpose the region determined in the presence of NSI. In this case, the theoretical best fit point lies almost exactly at the center of the ellipse-like region, thus offering a perfect description of the flat spectrum indicated by the current data. Therefore, the NSI scenario, respect to the standard MSW case, “gains” a negative $\Delta\chi^2 \sim -2.0$, which can be identified as the partial contribution arising from the better description of the solar energy spectrum to the total value ($\Delta\chi^2 \sim 3.6$) emerging from the global fit.

The remaining $\Delta\chi^2 \sim -1.6$ can be traced to the better agreement obtained in the presence of NSI, among the slightly different values of the mixing angle θ_{12} determined, respectively, by solar and KamLAND data (see Fig. 1). As discussed in [31, 36] this slight tension can be equally alleviated by the kinematical effects induced by non-zero values of the third mixing angle θ_{13} . It must be noted, however, that the observed flat behavior of the spectrum cannot be reproduced by a non-zero value of θ_{13} , since this parameter induces only an energy-independent suppression of the 2-flavor survival probability. Therefore, in the general three-flavor case we expect only a modest reduction of the statistical preference for NSI. The robustness of the hint is confirmed by numerical calculations, which allowing for $\theta_{13} > 0$, still indicate

a preference for NSI at the 1.5σ level. The future reactor searches [37] will provide a measurement of θ_{13} unaffected by (standard and non-standard) dynamical effects. Therefore, their negative (positive) result, will slightly favor (disfavor) the NSI hypothesis discussed here.

V. CONCLUSIONS

We have shown that the latest solar neutrino data (in combination with KamLAND) favor the presence of non-standard dynamical terms in the MSW Hamiltonian at a non negligible statistical level, thus hinting at new neutrino interactions. We have shown how such an indication, already present with lower statistical significance in older data, is now enhanced by the anomalous spectral behavior observed in three experiments. We stress that the indication we have discussed is indirect, and may be confused with other possible sources of anomalous spectral distortions, as those induced by conversions into new sterile neutrino states [38, 39]. Therefore, the identification of the correct sub-leading effect (if any) will need further corroboration not only from new indispensable low-energy solar neutrino measurements, but also from the remaining neutrino phenomenology.

Acknowledgments

We would like to thank A. Ianni for useful information on the Borexino detector. Our work is supported by the DFG Cluster of Excellence ‘Origin and Structure of the Universe’.

-
- [1] L. Wolfenstein, Phys. Rev. D **17**, 2369 (1978).
 - [2] S.P. Mikheev and A.Yu. Smirnov, Yad. Fiz. **42**, 1441 (1985) [Sov. J. Nucl. Phys. **42**, 913 (1985)].
 - [3] L. Wolfenstein, in *Neutrino ’78*, 8th International Conference on Neutrino Physics and Astrophysics (Purdue U., West Lafayette, Indiana, 1978), ed. by E.C. Fowler (Purdue U. Press, 1978), p. C3.
 - [4] J. N. Abdurashitov *et al.* (SAGE Collaboration), J. Exp. Theor. Phys. **95**, 181 (2002).
 - [5] W. Hampel *et al.* (GALLEX Collaboration), Phys. Lett. B **447**, 127 (1999).
 - [6] M. Altmann *et al.* (GNO Collaboration), Phys. Lett. B **616**, 174 (2005).
 - [7] T. Kirsten, J. Phys. Conf. Ser **120**, 052013 (2008).
 - [8] Q. R. Ahmad *et al.* (SNO Collaboration), Phys. Rev. Lett. **87**, 071301 (2001); **89**, 011301 (2002); **89**, 011302 (2002).
 - [9] S. N. Ahmed *et al.* (SNO Collaboration), Phys. Rev. Lett. **92**, 181301 (2004).
 - [10] B. Aharmim *et al.* (SNO Collaboration), Phys. Rev. C **72**, 055502 (2005).
 - [11] B. Aharmim *et al.* [SNO Collaboration], Phys. Rev. C **75**, 045502 (2007).
 - [12] B. Aharmim *et al.* (SNO Collaboration), Phys. Rev. Lett. **101**, 111301 (2008).
 - [13] B. Aharmim *et al.* [SNO Collaboration], Phys. Rev. C **81**, 055504 (2010).
 - [14] S. Fukuda *et al.* (Super-Kamiokande Collaboration), Phys. Rev. Lett. **86**, 5651 (2001); **86**, 5656 (2001).
 - [15] S. Fukuda *et al.* [Super-Kamiokande Collaboration], Phys. Lett. B **539**, 179 (2002).
 - [16] B. Yang [Super-Kamiokande Collaboration], arXiv:0909.5469 [hep-ex].
 - [17] B. T. Cleveland *et al.*, Astrophys. J. **496**, 505 (1998).
 - [18] C. Arpesella *et al.* [The Borexino Collaboration], Phys. Rev. Lett. **101**, 091302 (2008).
 - [19] G. Bellini *et al.* [The Borexino Collaboration], Phys. Rev. D **82**, 033006 (2010).
 - [20] K. Eguchi *et al.* [KamLAND Collaboration], Phys. Rev. Lett. **90**, 021802 (2003).
 - [21] T. Araki *et al.* [KamLAND Collaboration], Phys. Rev. Lett. **94**, 081801 (2005).

- [22] S. Abe *et al.* [KamLAND Collaboration], Phys. Rev. Lett. **100**, 221803 (2008).
- [23] A. Gando *et al.*, arXiv:1009.4771 [hep-ex].
- [24] J. W. F. Valle, Phys. Lett. B **199**, 432 (1987).
- [25] M. M. Guzzo, A. Masiero and S. T. Petcov, Phys. Lett. B **260**, 154 (1991).
- [26] E. Roulet, Phys. Rev. D **44**, R935 (1991).
- [27] A. Friedland, C. Lunardini and C. Pena-Garay, Phys. Lett. B **594**, 347 (2004).
- [28] M. Guzzo *et al.*, Nucl. Phys. B **629**, 479 (2002).
- [29] N. Fornengo, M. Maltoni, R. Tomas and J. W. F. Valle, Phys. Rev. D **65**, 013010 (2002).
- [30] M. C. Gonzalez-Garcia and M. Maltoni, Phys. Rept. **460**, 1 (2008).
- [31] A. Palazzo and J. W. F. Valle, Phys. Rev. D **80**, 091301 (2009).
- [32] W. A. Mann, D. Cherdack, W. Musial and T. Kafka, Phys. Rev. D **82**, 113010 (2010).
- [33] J. Kopp, P. A. N. Machado and S. J. Parke, Phys. Rev. D **82**, 113002 (2010).
- [34] G. L. Fogli *et al.*, Phys. Rev. D **78**, 033010 (2008).
- [35] S. Davidson, C. Pena-Garay, N. Rius and A. Santamaria, J. High Energy Phys. 03 (2003) 011; C. Biggio, M. Blennow and E. Fernandez-Martinez, J. High Energy Phys. 08 (2009) 090.
- [36] G. L. Fogli *et al.*, Phys. Rev. Lett. **101**, 141801 (2008).
- [37] F. Ardellier *et al.* (Double Chooz Collaboration), hep-ex/0606025; M. C. Chu (Daya Bay Collaboration), arXiv:0810.0807; Y. Oh (RENO Collaboration), Nucl. Phys. Proc. Suppl. **188** (2009) 109.
- [38] P. C. de Holanda and A. Y. Smirnov, Phys. Rev. D **69**, 113002 (2004).
- [39] P. C. de Holanda and A. Y. Smirnov, arXiv:1012.5627 [hep-ph].